Virology 433 (2012) 131–141

Contents lists available at SciVerse ScienceDirect

Virology

journal homepage: www.elsevier.com/locate/yviro

Identification of domains in p27 auxiliary replicase protein essential for its association with the endoplasmic reticulum membranes in *Red clover necrotic mosaic virus*

Kusumawaty Kusumanegara, Akira Mine, Kiwamu Hyodo, Masanori Kaido, Kazuyuki Mise, Tetsuro Okuno*

Laboratory of Plant Pathology, Graduate School of Agriculture, Kyoto University, Sakyo-ku, Kyoto 606-8502, Japan

ARTICLE INFO

Article history:
Received 27 May 2012
Returned to author for revisions
22 June 2012
Accepted 19 July 2012
Available online 14 August 2012

Keywords:
RNA replicase
RNA virus
RNA replication
ER membrane
Amphipathic α-helix
Tombusviridae
Dianthovirus
Membrane-flotation assay
Confocal microscopy

ABSTRACT

Positive-strand RNA viruses require host intracellular membranes for replicating their genomic RNAs. In this study, we determined the domains and critical amino acids in p27 of *Red clover necrotic mosaic virus* (RCNMV) required for its association with and targeting of ER membranes in *Nicotiana benthamiana* plants using a C-terminally GFP-fused and biologically functional p27. Confocal microscopy and membrane-flotation assays using an *Agrobacterium*-mediated expression system showed that a stretch of 20 amino acids in the N-terminal region of p27 is essential for the association of p27 with membranes. We identified the amino acids in this domain required for the association of p27 with membranes using alanine-scanning mutagenesis. We also found that this domain contains amino acids not critical for the membrane association but required for the formation of viral RNA replication complexes and negative-strand RNA synthesis. Our results extend our understanding of the multifunctional role of p27 in RCNMV replication.

Introduction

The replication of positive-strand RNA viruses is performed by viral replication complexes that consist of viral RNA-dependent RNA polymerase (RdRp), viral auxiliary proteins, host-encoded proteins, and viral RNAs on intracellular membranes in infected cells (Ahlquist et al., 2003; den Boon et al., 2010; Nagy and Pogany, 2012). Intracellular membranes utilized by plant RNA viruses differ, and include those of the endoplasmic reticulum (ER), chloroplasts, vacuoles, peroxisomes, and mitochondria (Ahlquist et al., 2003; Nagy and Pogany, 2008; Ritzenthaler and Elamawi, 2006; Salonen et al., 2005). Viral proteins play essential roles in targeting viral replication complexes to the membranes and induce morphological alterations of the membranes (den Boon et al., 2010; Miller and Krijnse-Locker, 2008). For example, the 1a protein of *Brome mosaic virus* (BMV) localizes to ER membranes, induces vesicular ER invaginations or spherules, and recruits RNA templates to the membranes together with 2a RdRp (den Boon et al., 2010; Liu et al., 2009; Schwartz et al., 2002, 2004; Wang et al., 2005). The auxiliary replicase protein p33 of the tombusviruses (*Tomato bushy stunt virus* and *Cucumber necrosis virus*) recruits a replicon RNA and p92 RdRp into the peroxisomal membranes in yeast, a model host for the study of virus replication (McCartney et al., 2005; Panavas et al., 2005). The replicase protein p36 of *Carnation Italian ringspot virus* (CIRV), another member of the tombusviruses, localizes to the outer mitochondrial membrane and induces the formation of multivesicular bodies (Hwang et al., 2008; Rubino et al., 2001; Weber-Lotfi et al., 2002). Turnip yellow mosaic virus 140 K replication protein mediates the targeting of another 66 K replication protein with RdRp motif to the chloroplast envelope (Prod'homme et al., 2003). Domains essential for membrane association have been identified in the replication proteins of several viruses, including BMV 1a (den Boon et al., 2001; Liu et al., 2009; Schwartz et al., 2002), p33 and p36 of the tombusviruses (Hwang et al., 2008; Navarro et al., 2004; Panavas et al., 2005), tobacco etch virus 6 K protein (Schaad et al., 1997), tobacco mosaic virus 126 kDa protein (dos Reis Figueira et al., 2002), tomato ringspot nepovirus NTB-VPg and X2 proteins (Zhang et al., 2005; Zhang and Sanfaçon, 2006), poliovirus 2C and 3AB proteins (Echeverri and Dasgupta, 1995; Teterina et al., 1997; Towner and Semler, 1996), Hepatitis C virus (HCV) nonstructural proteins NS5A and NS5B (Brass et al., 2002; Schmidt-Mende et al., 2001), and flock house virus protein A (Van Wynsberghe et al., 2007).

Red clover necrotic mosaic virus (RCNMV) is a positive-sense single-stranded RNA plant virus with a bipartite genome and

* Corresponding author. Fax: 81 75 753 6131.
E-mail address: okuno@kais.kyoto-u.ac.jp (T. Okuno).

0042-6822/$ - see front matter © 2012 Elsevier Inc. All rights reserved.
http://dx.doi.org/10.1016/j.virol.2012.07.017

a member of the genus *Dianthovirus* in the family *Tombusviridae*. Both genomic RNAs lack a 5′ cap structure (Mizumoto et al., 2003) and a 3′ poly(A) tail (Lommel et al., 1988; Mizumoto et al., 2003; Xiong and Lommel, 1989). RNA1 (3.9 kb) encodes N-terminally overlapping replicase proteins, a 27 kDa protein (p27) and an 88 kDa protein (p88). p88 contains an RdRp motif (Koonin, 1991) produced by programmed-1 ribosomal frameshifting (Kim and Lommel, 1994; Tajima et al., 2011; Xiong et al., 1993) and is required in *cis* for RNA1 replication (Okamoto et al., 2008). RNA1 also encodes a 37 kDa coat protein that is translated from subgenomic RNA (Zavriev et al., 1996). RNA2 (1.5 kb) encodes a 35 kDa movement protein (MP) that is required for cell-to-cell movement in plants (Xiong et al., 1993).

The auxiliary replicase protein p27 of RCNMV, together with p88 and some host proteins, forms the 480 kDa viral replicase complex associated with ER membranes in RCNMV-infected cells (Mine et al., 2010a). Assembly of the 480 kDa complexes requires both p27–p27 and p27–p88 interactions, in which the C-terminal region of p27 and the nonoverlapping region unique to p88 are involved (Mine et al., 2010b). p27 also plays an essential role in the recruitment of RNA2 to ER membranes via binding to a Y-shaped RNA element (YRE) in the 3′ noncoding region of RNA2 (Iwakawa et al., 2011). The domains and critical amino acids required for RNA binding were mapped to the central and the C-terminal regions of p27 (Hyodo et al., 2011). A preceding study with confocal microscopy using N-terminally green fluorescent protein (GFP)-fused p27 (GFP-p27) and p88 (GFP-p88) revealed that both proteins colocalize to the cortical and cytoplasmic ER, and that p27 causes ER membrane restructuring and proliferation (Turner et al., 2004). However, the relationship between the protein localization and the formation of a functional replication complex remains elusive.

In this study, we determined the domains and critical amino acids in p27 required for its association with and targeting of ER membranes using a C-terminally GFP-fused p27 (p27-GFP) that supports viral RNA replication in the presence of p88. Confocal microscopy and membrane-flotation assays revealed that the membrane association of p27 is mediated by a stretch of 20 amino acids located in the N-terminal region of p27 (amino acids 31–50) and that the 20 amino acid sequence is sufficient for targeting nonviral GFP to ER membranes. Mutations that impeded the membrane association of p27 compromised the formation of RCNMV RNA replication complexes and negative-strand RNA synthesis.

Results and discussion

p27-GFP supports RCNMV RNA replication in the presence of p88 and localizes to ER membranes

First, to obtain a biologically functional GFP-fused p27, we constructed N-terminally GFP-fused p27 (GFP-p27) and C-terminally GFP-fused p27 (p27-GFP) (Fig. 1A), and tested their ability to support the replication of RNA2 by coexpression with p88 and RNA2 using an *Agrobacterium*-mediated expression system (agroinfiltration) in *Nicotiana benthamiana* (Takeda et al., 2005). Accumulations of viral proteins and RNAs were analyzed by western and northern blotting methods, respectively, at 2 days after infiltration (dai). p27-GFP, but not GFP-p27, accumulated and supported the accumulation of both negative and positive-strand RNA2 (Fig. 1B). These results indicate that p27-GFP is biologically functional. In contrast, GFP-p27 seems to be unstable and non-functional in our experimental system. The mRNA levels of GFP-p27 and p27-GFP were similar when assessed by RT-PCR using total RNA isolated from *Agrobacterium*-infiltrated leaves expressing GFP-p27 or p27-GFP in the presence of p88 and RNA2 (data not shown). Moreover, C-terminally DsRed-monomer (DRm)-fused p27 (p27-DRm) was more stable than N-terminally DRm-fused p27 (DRm-p27) and only p27-DRm supported RCNMV RNA replication (K. Kusumanegara and T. Okuno, unpublished data). Therefore, we used p27-GFP in further experiments.

In a previous study, N-terminally GFP-fused p27 was successfully used to investigate intracellular localization of p27 (Turner et al., 2004). The success could be attributed to the experimental system, in which the fusion protein was expressed from RCNMV RNA1 or a viral vector, or expressed from a plasmid vector via microprojectile bombardment.

We investigated the subcellular localization of p27-GFP in the agroinfiltrated *N. benthamiana* leaves using a confocal laser scanning microscopy. The fluorescence of p27-GFP was observed as large aggregates in most of the cells observed, and these fluorescent areas merged well with those of an ER marker at 2 dai (Fig. 1C, upper panels). The fluorescence of p27-GFP was also observed to merge with that of the ER marker in the cortical and perinuclear regions but was not observed inside the nucleus (data not shown). The patterns of observed fluorescence of p27-GFP were similar at 2, 3, and 4 dai (data not shown). In contrast, the fluorescence of free GFP was observed in the cytoplasm and these fluorescent areas did not coincide with those of an ER marker (Fig. 1C, lower panels). The fluorescence of free GFP was also observed inside the nucleus of leaf epidermal cells (Fig. 1C, lower panels, and data not shown). These observations suggest that p27-GFP colocalizes with the ER membranes and that p27-GFP disrupts a normal reticular structure of cortical ER by inducing membrane restructuring and proliferation, as reported previously by Turner et al. (2004).

Next, we investigated the subcellular localization of p27-GFP in the presence of p88 and RNA2. At 2 dai, small fluorescent punctates were observed along ER filaments in most cells and large aggregates were barely detected (Fig. 1C, middle panels). Later at 3 and 4 dai, larger aggregates associated with the proliferated ER adjacent to the nucleus were detected in many cells (data not shown). Transition of localization pattern of p27-GFP is similar to that of the fusion protein of RCNMV MP and GFP (MP-GFP) in *N. benthamiana* epidermal cells and protoplasts infected with the recombinant virus expressing the MP-GFP (Kaido et al., 2009). The small punctates might be a progressive form of RNA replication complexes. The significance of the difference between the small punctates and large aggregates was not further addressed in this study.

Domains in p27 essential for its subcellular localization and association with the ER membranes

To determine domain(*s*) of p27 essential for its subcellular localization and association with the ER membranes, we expressed the GFP-fused N-terminal half of p27 (p27N1–113-GFP) and GFP-fused C-terminal half of p27 (p27N114–236-GFP) together with an ER marker in *N. benthamiana* leaves and observed their subcellular localization, as described above. Fluorescence of p27N1–113-GFP was observed as small aggregates and punctate spots in the cytoplasm and merged well with the ER marker (Fig. 2C). Expression of p27N1–113-GFP similar to p27-GFP induced morphological alteration of cortical ER, although the size of aggregates appeared to be smaller than that of the aggregates induced by wild-type p27-GFP (Fig. 2B and C). In contrast, expression of p27N114–236-GFP, similar to wild-type free GFP, appeared not to induce the morphological alteration of ER. In addition, similar to wild-type free GFP, the fluorescence of p27N114–236-GFP dispersed in the cytoplasm and barely merged with the fluorescence of the ER marker (Fig. 2A and D). These results indicate that the N-terminal half of p27 is responsible for its membrane association.

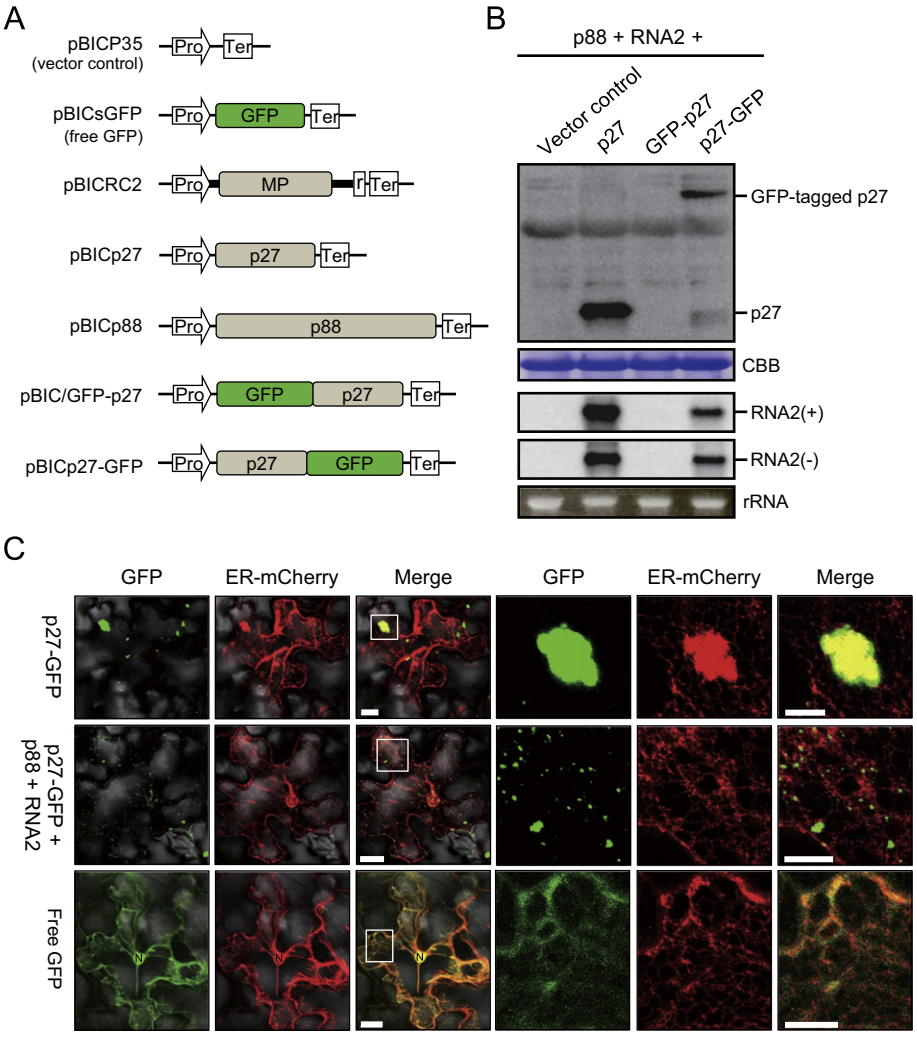

Fig. 1. p27-GFP is biologically functional and localizes to the ER membranes. (A) Schematic representation of the expression cassettes of plasmids used for agroinfiltration experiments in *N. benthamiana* leaves. Light shaded boxes denote ORFs of RCNMV and bold lines denote untranslated region of RCNMV RNA2. Green boxes denote synthetic green fluorescent protein. Key: Pro, *Cauliflower mosaic virus* (CaMV) 35S promoter; Ter, CaMV 35S terminator; r, the ribozyme sequence of *Tobacco ringspot virus* satellite RNA. (B) Western and northern blot analyses of total protein and total RNA extracted from leaves 2 days after infiltration (2 dai). p27 and GFP-tagged p27 were detected using a rabbit polyclonal antibody raised against p27. Accumulations of viral RNAs were detected using specific riboprobes. Coomassie brilliant blue-stained proteins (CBB) and ethidium bromide-stained rRNAs (rRNA) are shown below the western blots and northern blots, respectively, to represent the loading controls. (C) Subcellular localization of p27-GFP in the absence and presence of p88 and RNA2 in *N. benthamiana* epidermal cells (2 dai). pBIC/ER-mCherry (Kaido et al., 2011) was coinfiltrated as the ER marker. At 2 dai, the infiltrated leaves were subjected to confocal microscopy. Confocal projections composed of at least 15 optical sections taken at 1 μm intervals, covering from the surface to the middle of epidermal cells. N: nucleus; scale bar=20 μm; scale bar for zoomed images=10 μm.

To delimit the region in the N-terminal half of p27 required for the membrane association, we constructed p27N1–113-GFP derivatives with a series of deletions, and analyzed their subcellular localization in agroinfiltrated *N. benthamiana* leaves. Fluorescence of p27N21–113-GFP, p27N31–113-GFP, p27N31–80-GFP, p27N31–60-GFP, and p27N31–50-GFP merged well with that of the ER marker (Fig. 2E and G, data not shown). Unlike p27-GFP (Fig. 1C, upper panels, and Fig. 2B), the fluorescent signals by these p27N1–113-GFP derivatives were detected as small punctates or web-like structures (Fig. 2E, G, and data not shown). In contrast, fluorescence of p27N41–113-GFP and p27N21–40-GFP scarcely merged with that of an ER marker (Fig. 2F and H). The ability of p27N31–50-GFP to target the ER membranes suggested that a stretch of 20 amino acids in the N-terminal region of p27 (amino acids 31–50) is essential and sufficient for targeting GFP to the ER membranes (Fig. 2G). Interestingly, p27Δ31–50-GFP, in which the 20 amino acids had been deleted, formed small punctates, and they were located along ER filaments (Fig. 2I). However, this mutant did not induce large aggregate structures (Fig. 2I, data not shown). These results suggest that the formation of small punctate structures by the mutant p27 might be independent of morphological alteration of ER membranes.

To investigate more precisely and confirm the association of p27 with intracellular membranes and the importance of the 20 amino acid sequence in the membrane association, we performed membrane-flotation assays (Sanfaçon and Zhang, 2008). The postnuclear fractions (see Materials and Methods) prepared from *Agrobacterium*-infiltrated leaves expressing p27-GFP, p27-FLAG, p27N31–50-GFP, p27Δ31–50-GFP (Fig. 3A), or free GFP were fractionated using a two-step sucrose-centrifugation gradient and subjected to SDS-PAGE/western blot analysis. p27-GFP, p27-FLAG, and p27N31–50-GFP were fractionated at the interface between the 10% and 65% sucrose solution that is expected to contain membrane-associated proteins (Fig. 3B), while free GFP and p27Δ31–50-GFP remained at the bottom of the gradient (Fig. 3B and C). Thus, we concluded that p27-GFP is a membrane-associated protein and that the 20 amino acid sequence ($_{31}$CNLGIDCWNRFRKWFFGLNF$_{50}$) in the N-terminal region of p27 is essential and sufficient for the association of p27

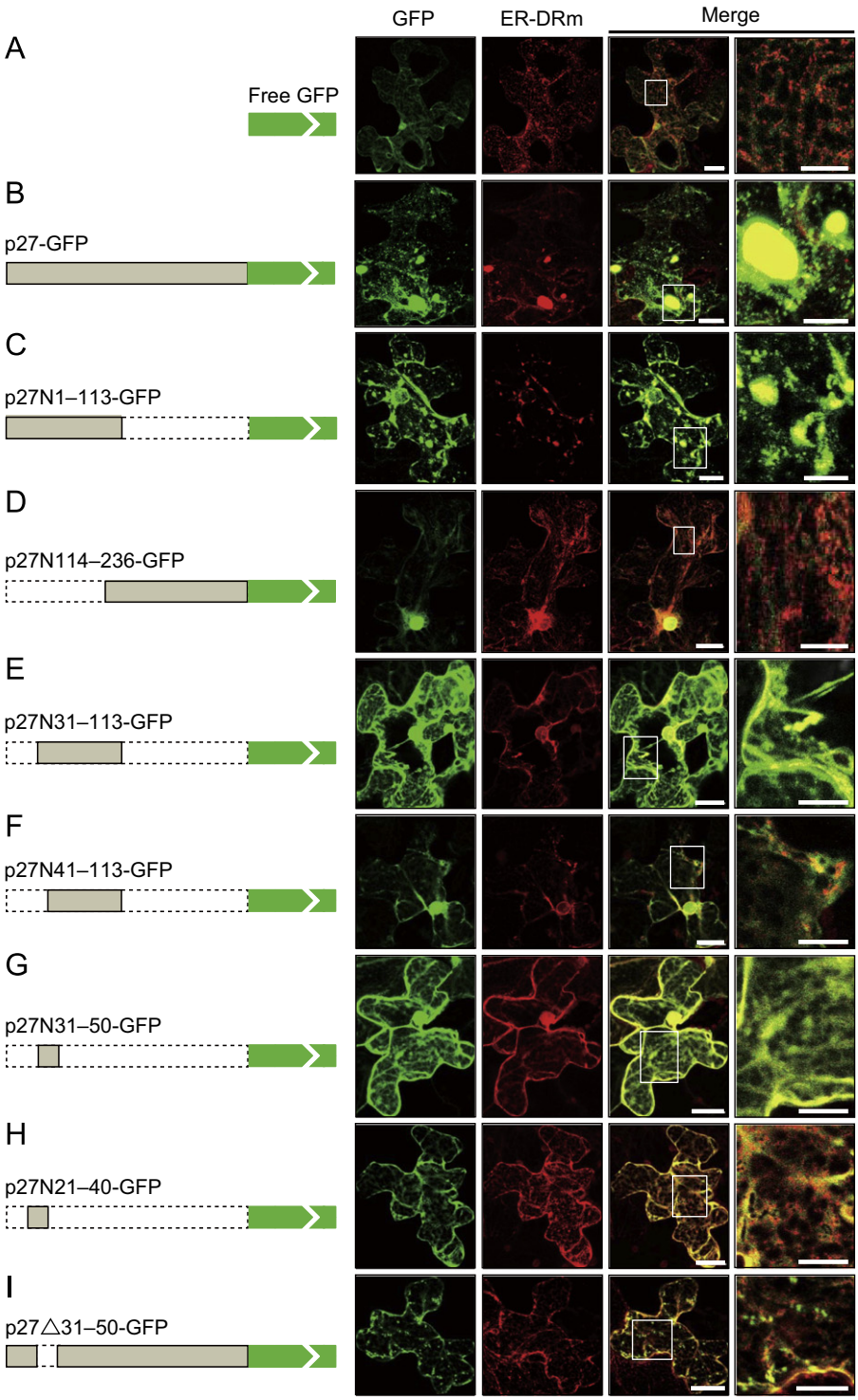

Fig. 2. Subcellular localization of deletion mutants of p27-GFP in *N.* benthamiana epidermal cells. pBIC/ER-DRm (Kaido et al., 2009) was coinfiltrated as the ER marker. Scale bar=20 μm; scale bar for zoomed images=10 μm. For others, see the legend of Fig. 1C.

with membranes. The 20 amino acid sequence of p27 is highly conserved among dianthoviruses (Fig. 4A). We name this 20 amino acid sequence the membrane-association domain of p27.

Amino acids critical for the association of p27 with membranes

To specify amino acids that contribute to the association of p27 with membranes, we performed alanine-scanning mutagenesis in the membrane-association domain of p27-GFP. We constructed nine p27-GFP mutants with hydrophobic amino acids (Fig. 4A) substituted for alanine. *Agrobacterium*-infiltrated leaves expressing mutant proteins were subjected to a membrane-flotation assay (Fig. 4B). p27/W38A-GFP and p27/F41A-GFP were dispersed in the gradient and predominantly detected at the bottom of the gradient. A double mutation of W38 and F41 to alanine impeded the membrane association of the mutant p27 (p27/W38A F41A-GFP) much more severely compared with single mutations (Fig. 4B). These results suggest that the tryptophan at

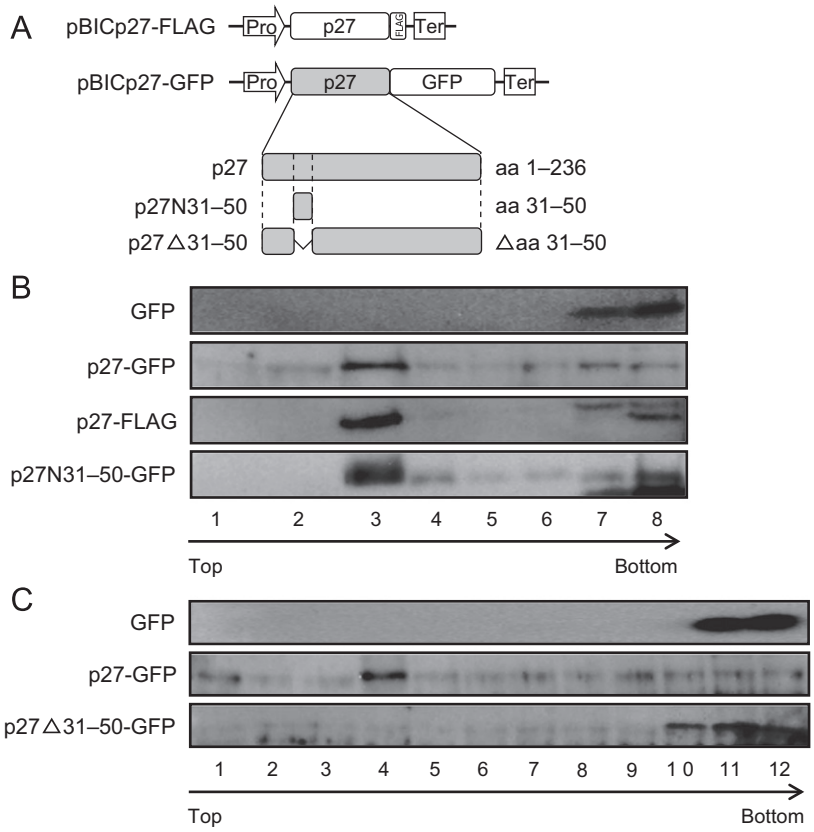

Fig. 3. Membrane-flotation assays of p27 fusion proteins. Equal volumes of postnuclear fractions derived from *Agrobacterium*-infiltrated leaves (2 dai) expressing p27-GFP, p27-GFP deletion mutants, or p27-FLAG were subjected to membrane-flotation assays. Fractions were collected from a two-step sucrose gradient, and proteins in each collected fraction were subjected to SDS-PAGE/western blot analysis. (A) Schematic representation of the expression cassettes of plasmids used for agroinfiltration experiments in *N. benthamiana* leaves. (B) Membrane-flotation assays of p27-GFP, p27-FLAG, and p27N31–50-GFP. p27-GFP was detected using a rabbit polyclonal antibody raised against p27. GFP and p27N31–50-GFP were detected using LivingColors A.v. Peptide antibody (Clontech). p27-FLAG was detected using anti-FLAG M2 monoclonal antibody (Sigma-Aldrich). (C) Membrane-flotation assays of p27-GFP and p27Δ31–50-GFP. Proteins were detected using Living Colors A.v. Peptide antibody (Clontech).

position 38 (W38) and phenylalanine at position 41 (F41) play essential roles in the association of p27-GFP with membranes. A main band of p27/F45A-GFP was consistently detected in the upper fraction compared with the wild-type p27-GFP (Fig. 4B). This finding will be discussed later.

Using the secondary structure prediction server Jpred 3 (Cole et al., 2008), the membrane-association domain of p27 is predicted to be predominantly α-helical (Fig. 5A). A helical wheel projection (Schiffer and Edmundson, 1967) of the 18 amino acid sequence (amino acids 30–47) that includes most of the membrane-association domain (amino acids 31–50) suggests that this region has the potential to form an amphipathic α-helix with one side having a cluster of hydrophilic, polar residues and the other side hydrophobic, nonpolar residues including W38 and F41 (Fig. 5B). This result supports the role of W38 and F41 in membrane association.

Nonstructural viral proteins with hydrophobic sequences may transverse the membrane similar to polytopic integral membrane proteins: nonstructural proteins NS2 and NS4B of Hepatitis C virus (HCV) are integral polytopic membrane proteins (Gouttenoire et al., 2010; Yamaga and Ou, 2002). It is also known that viral nonstructural proteins, such as BMV 1a and semliki forest virus nsP1, interact with membranes monotopically as a peripheral membrane protein via an amphipathic α-helical peptide that enables their membrane integration or interaction (Liu et al., 2009; Salonen et al., 2005; Schwartz et al., 2004; Spuul et al., 2007). Meanwhile, an amino-terminal amphipathic α-helix mediates membrane association of HCV NS5A as an integral membrane protein (Brass et al., 2002).

Our previous study suggested that p27 and p88 associate tightly with ER membranes as a 480 kDa complex in RCNMV-infected cells (Mine et al., 2010a). To determine whether p27 protein alone can associate tightly with ER membranes, we prepared solubilized membrane fractions from *Agrobacterium*-infiltrated leaves expressing p27-GFP and treated the fractions with 1 M potassium chloride, 0.1 M sodium carbonate (pH 11), or 4 M urea, as described previously (Mine et al., 2010a; Sanfaçon and Zhang, 2008). None of these treatments significantly released p27 from the membrane fraction (data not shown), affirming a tight association of p27 with the ER. These results suggest that p27 associates with ER membranes as an integral monotopic protein that is attached from one side and forms an amphipathic α-helix constituted by amino acids including W38 and F41 in its N-terminal region.

Effects of mutations in the membrane-association domain of p27 on the formation of RCNMV RNA replication complexes

Our previous studies demonstrated that RCNMV replicase proteins form the 480 kDa complex that contains p27, p88, and several host proteins (Mine et al., 2010a). To investigate the effects of mutations in the membrane-association domain of p27 on the formation of RCNMV RNA replication complexes, we analyzed the accumulation of the viral replication complexes in *Agrobacterium*-infiltrated leaves expressing p27-GFP or its mutants together with p88 and RNA2 using blue-native polyacrylamide gel electrophoresis (BN/PAGE) and SDS-PAGE followed by western blotting, as previously described (Mine et al., 2010a).

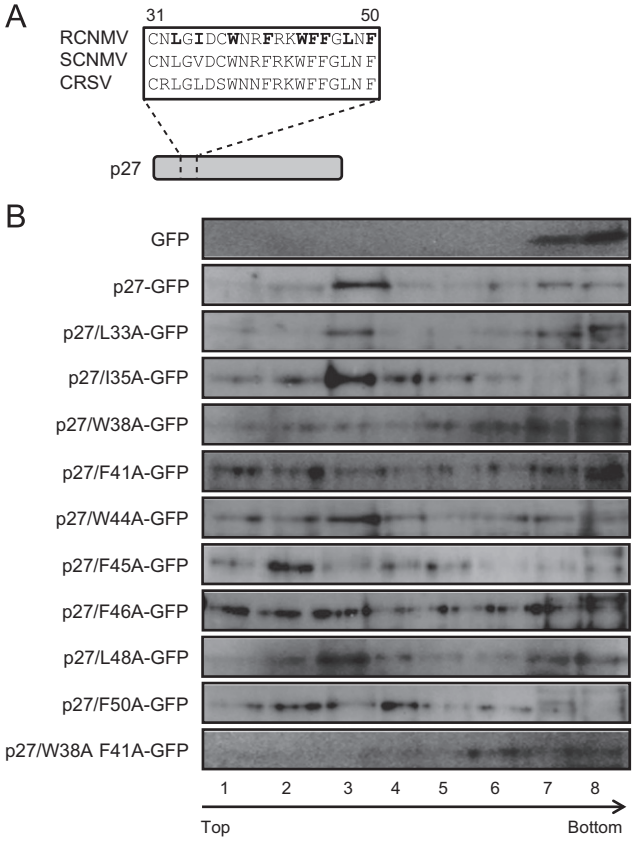

Fig. 4. Membrane-flotation assays of alanine-scanning mutants of p27-GFP. (A) Sequence alignments of the membrane-association domain in p27 of RCNMV and other dianthoviruses. The conserved amino acids selected for alanine-scanning mutagenesis are shown with bold-faced letters. SCNMV: *Sweet clover necrotic mosaic virus*; CRSV: *Carnation ringspot virus*. For agroinfiltration experiments in *N. benthamiana* leaves, the GFP domain is fused to the C-terminal of each p27 mutant. (B) Membrane-flotation assays of alanine-scanning mutants of p27-GFP. p27-GFP and its mutants were detected using a rabbit polyclonal antibody raised against p27. GFP was detected using Living Colors A.v. Peptide antibody (Clontech). For others, refer to the legend of Fig. 3.

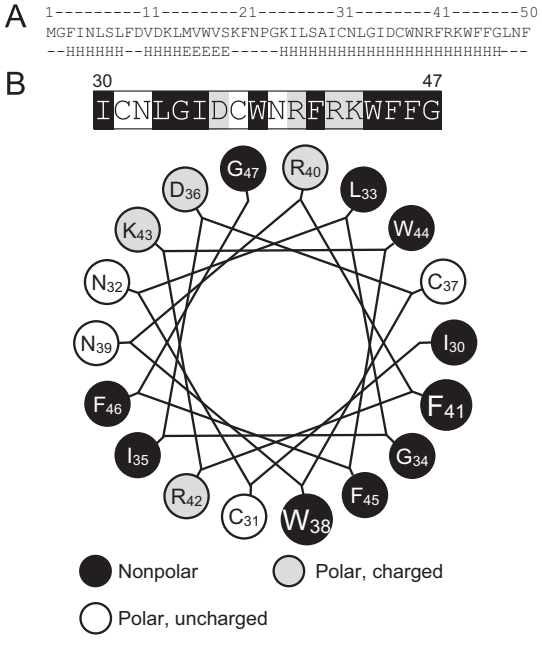

C

	p27	L33A	I35A	W38A	F41A	W44A	F45A	F46A	L48A	F50A	W38A /F41A
Membrane-association	+	+	+	+/-	+/-	+	+	+	+	+	-
RNA replication	+	+	+	-	-	+	-	-	-	-	-

Fig. 5. (A) Computer-assisted secondary structure prediction (Jpred 3) (Cole et al., 2008) of N-terminal region in p27 protein (amino acids 1–50). (B) Linear and helical wheel projections of the 18 amino acid sequence including most of the membrane-association domain of p27. One side of the predicted amphipathic α-helix has predominantly hydrophobic, nonpolar residues, while the opposite side has hydrophilic, polar residues. (C) The membrane association and RNA replication of alanine-scanning mutants of p27. See Figs. 4, 6 and 7.

A predicted molecular mass of RNA replication complexes formed with p27-GFP should be twice as large as those formed with p27 because the molecular weight of GFP is similar to that of p27. Complexes with molecular mass of approximately 850 kDa, based on their migration pattern, accumulated in leaves expressing p27-GFP, p27/L33A-GFP, p27/I35A-GFP, and p27/W44A-GFP, whereas other p27-GFP mutants failed to accumulate the 850 kDa complexes (Fig. 6). Northern blot analysis showed that the accumulated levels of viral RNAs reflected those of the 850 kDa complexes (Fig. 6). Interestingly, there are two types of p27-GFP mutants that failed to support the accumulation of 850 kDa complexes.

One type includes p27/F46A-GFP, p27/L48A-GFP, and p27/F50A-GFP. These mutants accumulated to levels similar to those of p27-GFP (Fig. 6) and retained the ability to associate with cellular membranes as assessed by membrane-flotation assays (Fig. 4B). These results suggest that the membrane-association domain of p27 is involved in a function(s) of p27 other than membrane association in viral RNA replication. Considering that the N-terminal half of p27 is not essential for the interactions with p27 and p88 (Mine et al. 2010b), these amino acids (F46, L48 and F50) might be involved in the interaction with host protein(s) associated with RCNMV RNA replication complexes (Mine et al., 2010a). In HCV, amino acid substitutions within the membrane-insertion sequence of NS5B abolish viral RNA replication without affecting its membrane association, indicating that the C-terminal domain of NS5B has functions beyond serving as a membrane anchor and suggesting that this domain could be involved in critical intramembrane protein–protein interactions (Moradpour et al., 2004).

Other types of mutants include p27/W38A-GFP, p27/F41A-GFP, and p27/F45A-GFP that poorly accumulated in the infiltrated leaves (Fig. 6). p27/W38A-GFP and p27/F41A-GFP did not associate well with cellular membranes as assessed by membrane-flotation assays (Fig. 4B). Loss of function in membrane association may explain their instability in the infiltrated leaves of *N. benthamiana*.

Instability of p27/F45A-GFP remains elusive, because p27/F45A-GFP behaved similar to a membrane-association protein in a membrane-flotation assay, although p27/F45A-GFP was fractionated into a different fraction from that of wild-type p27-GFP (Fig. 4B). It should be noted that F45 is positioned on the same side of F41 and W38 in a helical wheel projection in the predicted amphipathic α-helix (Fig. 5B). The F45A substitution mutation may affect the interaction of p27 with membranes or other factors required for the formation of RNA replication complexes, directly or indirectly. This remains to be solved.

Finally, we investigated the effects of mutations in the membrane-association domain of p27 on the formation of RNA replication complexes using an in vitro assay system prepared from an evacuolated tobacco BY-2 protoplast lysate (BYL) (Komoda et al., 2004). Transcripts for p27-FLAG or its mutants and those for p88 were incubated with RNA2 in BYL and the accumulation of viral replication complexes and viral RNAs were analyzed, as described above. The effects of mutations on the

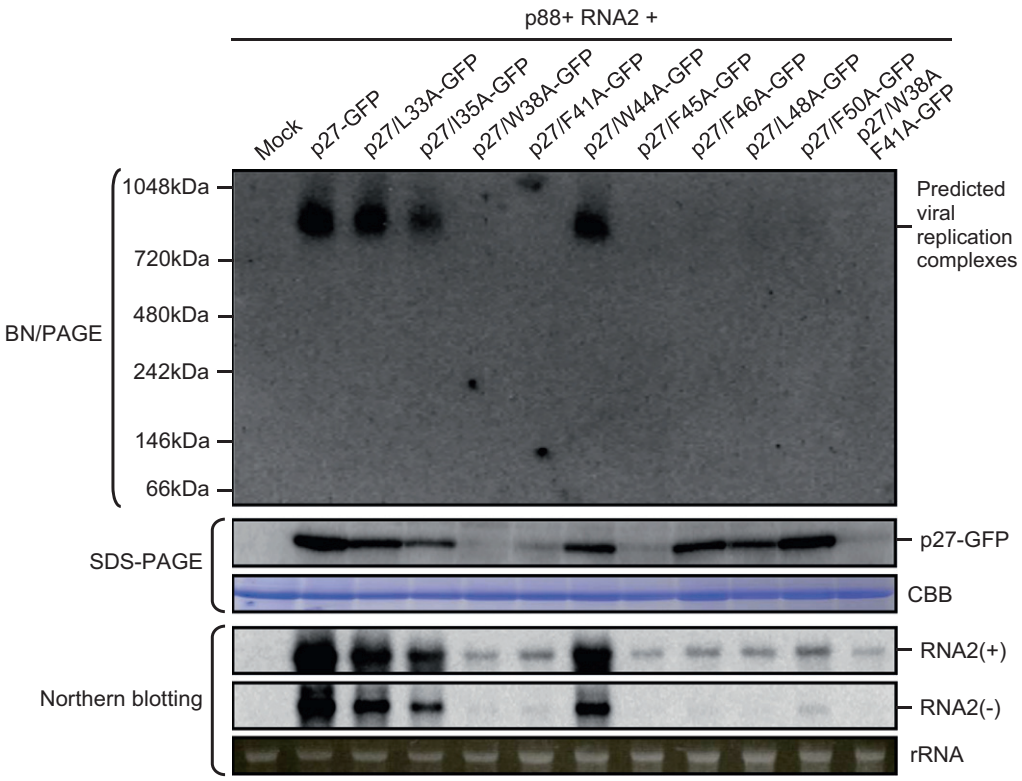

Fig. 6. Effects of alanine-scanning mutations introduced into p27 on the formation of the viral replication complexes and viral RNA accumulations. Upper panel is the accumulations of the viral replication complexes in *Agrobacterium*-infiltrated leaves (2 dai) expressing p27-GFP or its mutants in the presence of p88 and RNA2. The solubilized membrane fractions were subjected to BN/PAGE and SDS-PAGE followed by western blot analysis using a rabbit polyclonal antibody raised against p27. Accumulation of positive- and negative-strand RCNMV RNA2 in the leaves was analyzed by northern blot analysis using specific riboprobes. CBB and rRNA represent the loading controls.

accumulation of the 480 kDa complex and negative-strand RNA2 were similar to those obtained in *N. benthamiana* leaves using p27-GFP and its mutants, although all p27-FLAG mutants accumulated to a level similar to that of wild-type p27-FLAG (Fig. 7). These results indicate that none of the mutations introduced into p27-FLAG affected the stability of the proteins in BYL, at least during 4 h of incubation.

Conclusions

Our present study demonstrated that p27 associates with intracellular membranes via a membrane-association domain with an amphipathic α-helix predicted in the N-terminal region, and that the membrane association of p27 is essential, but not sufficient, for the formation of RCNMV RNA replication complexes and viral RNA replication. The domain also contains amino acids that are not critical for membrane association, but are required for the formation of RNA replication complexes (Fig. 5C). Thus, the 20 amino acid sequence in the membrane-association domain with an amphipathic α-helix is involved in multiple functions of p27 in the RNA replication of RCNMV.

Materials and methods

Plasmid construction

Plasmids containing the prefix 'pUC' and 'pBIC' were used for in vitro transcription and agroinfiltration, respectively. pUCR1 and pRC2|G are full-length cDNA clones of RCNMV Australian strain RNA1 and RNA2, respectively (Takeda et al., 2005; Xiong and Lommel, 1991). pUCR1-MsG was previously described (Kaido et al., 2009). pUCp27-FLAG and pUCp88 were described by Mine et al. (2010a, 2010b). pBICP35, pBICRC2, pBICp27, pBICp88, and pBICGFP were described in detail by Takeda et al. (2005). pBIC/ER-DRm and pBIC/ER-mCherry were previously described (Kaido et al., 2009, 2011). All plasmids generated in this study were PCR amplified using KOD-Plus-version 2 DNA polymerase (Toyobo, Osaka, Japan), ligated using DNA Ligation Kit version 2.1 (Takara Bio, Shiga, Japan), and verified by sequencing. The primers and their sequences used in this study are listed in Table 1.

To generate pBIC/GFP-p27, the entire coding region of sGFP was amplified from pUCR1-MsG using Bam/sGFP-R and p27/sGFP-L and the entire coding region of p27 was amplified from pUCR1 using sGFP/p27-R and Kpn/p27-L. A DNA fragment was then amplified from the mixture of these first-round DNA fragments using Bam/sGFP-R and Kpn/p27-L. The amplified DNA fragment was digested with *Bam*HI and *Kpn*I, and inserted into pBICP35 previously digested with the same restriction enzymes.

To generate pBICp27-GFP, the entire coding region of p27 was amplified from pBICp27 using *Bam*HIp27-F and sGFP-p27-R, and the entire coding region of sGFP was amplified from pBIC/GFP-p27 using p27-sGFP-F and *Kpn*I-sGFP2-R. A DNA fragment was then amplified from the mixture of these first-round ;DNA fragments using *Bam*HIp27-F and *Kpn*I-sGFP2-R. The amplified DNA fragment was digested with *Bam*HI and *Kpn*I, and inserted into pBIC/GFP-p27 previously digested with the same restriction enzymes.

To obtain all of the deletion mutants of pBICp27-GFP, DNA fragments were generated from pBICp27-GFP by overlapping PCR

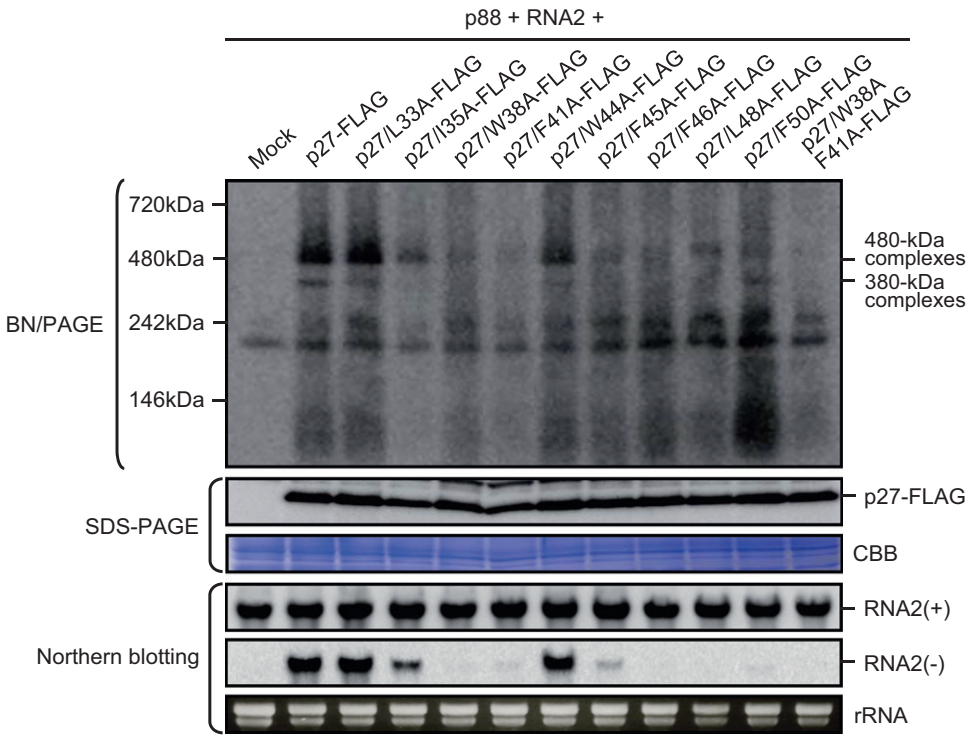

Fig. 7. Effects of alanine-scanning mutations introduced into p27 on the formation of the viral replication complexes and negative-strand RNA synthesis. Upper panel is the accumulations of the viral replication complexes in BYL incubated for 4 h with transcripts expressing p27-FLAG or its mutants in the presence of p88 and RNA2. The solubilized membrane fractions were subjected to BN/PAGE and SDS-PAGE followed by western blot analysis using an anti-FLAG M2 monoclonal antibody. Lower panel is the accumulations of negative-strand RNAs in total RNA analyzed by northern blot analysis using specific riboprobes. CBB and rRNA represent the loading controls.

using the primer pairs listed, digested with *Bam*HI and *Kpn*I, and ligated into the corresponding region of pBIC/GFP-p27.

Alanine-scanning mutants of pUCp27-FLAG and pBICp27-GFP were generated by site-directed mutagenesis using the primer pairs H*xx*A-F and H*xx*A-R, where *xx* refers to the position number of the mutated hydrophobic amino acid in the p27 protein. A total of 10 clusters of hydrophobic amino acid residues identified in the N-terminal region of p27 (amino acids 31–50) were changed to alanine. All of the derivative mutants of pBICp27-GFP were generated in a similar manner to that for pBICp27-GFP. To obtain all of the derivative mutants of pUCp27-FLAG, DNA fragments were amplified from pUCp27-FLAG. The primer pairs used were pUC*Sac*I-F and one each of the reverse primer listed. Another FLAG-*Mlu*I-R was used together with one each of the forward primer listed. Each recombinant PCR product was amplified by using pUC*Sac*I-F and FLAG-*Mlu*I-R, digested with *Sac*I and *Mlu*I, and inserted into the corresponding region of pUCp27-FLAG.

Plant growth conditions

N. benthamiana plants were grown on commercial soil (Tsuchi–Taro; Sumirin–Nosan–Kogyo, Tobishima, Aichi, Japan) at 25 ± 2 °C and 16 h illumination per day (Kaido et al., 2011). Six-week-old plants were used for agroinfiltration.

Agroinfiltration

N. benthamiana plants and *Agrobacterium tumefaciens* GV3101 (pMP90) were used for infiltration experiments, as previously described (Takeda et al., 2005). Total *Agrobacterium* cultures were suspended in 10 mM $MgCl_2$ to an OD_{600} of 0.8. GFP-tagged p27 or its mutants were individually infiltrated for membrane-flotation assays, coinfiltrated with pBIC/ER-mCherry or pBIC/ER-DRm for colocalization analyses, or coinfiltrated with pBICp88 and pBICRC2 for protein and RNA accumulation analyses.

Confocal microscopy

GFP and mCherry or DsRed-monomer fluorescence were observed using an Olympus FluoView FV500 confocal laser scanning microscope (Olympus Optical, Tokyo, Japan), as described by Kaido et al. (2011).

Subcellular fractionation and membrane-flotation assays

Subcellular fractionation and membrane-flotation assays were conducted essentially as previously described by Sanfaçon and Zhang (2008), with minor modifications. *Agrobacterium*-infiltrated leaves (2 dai) were gently ground into fine powder in liquid nitrogen, extracted in three volumes of homogenization buffer (50 mM Tris–HCl, pH 8, 10 mM KCl, 3 mM $MgCl_2$, 1 mM EDTA, 1 mM DTT, 0.1% BSA, 0.3% dextran, 13% (w/v) sucrose, and Complete Mini Protease Inhibitor Cocktail [Roche Applied Science, Mannheim, Germany; one tablet/10 mL; stored at −80 °C in 1.5 mL aliquots]) using a mortar and pestle, and centrifuged at $3{,}700 \times g$ for 10 min at 4 °C to discard nuclei, cell wall debris, and large organelles. The supernatant was collected as postnuclear fractions and transferred to a clean centrifuge tube. The postnuclear fractions (300 μL) were then mixed with 1.6 mL of 85% sucrose (the final concentration of sucrose will be 71.5%) and the mixture placed at the bottom of a 12 mL swinging-bucket centrifuge tube (13 PET Tube; Hitachi Koki, Tokyo, Japan). The mixture was overlaid with 7 mL of 65% sucrose and then 3.1 mL of 10% sucrose. After centrifugation at $100{,}000 \times g$ for 18 h at 4 °C, 8–1.5 mL or 12–1 mL fractions were collected from the top of the tube and subjected to SDS-PAGE/western blot analysis.

Table 1
List of primers and their sequences used for PCR to generate constructs described in the text

Primer name	Sequence
Bam/sGFP-R	GGGGATCCGGATGCATCATCATCATCATCATGTG
p27/sGFP-L	ATTTATAAAACCCATGCCCCCCTTGTACAGCTCGTCCATG
sGFP/p27-R	TGGACGAGCTGTACAAGGGGGGCATGGGTTTTATAAATCTTTC
Kpn/p27-L	GGGGTACCCTAAAAATCCTCAAGGGATTT
p27-sGFP-F	TTTTGGGGGCATGCATCATCATCATCATCATGTGA
sGFP-p27-R	GATGATGCATGCCCCCAAAATCCTCAAGGGATTTG
*Kpn*I-sGFP2-R	GCGGGGTACCCTACTTGTACAGCTCGTCCA
*Bam*HI-p27-F	GGGGATCCGGATGGGTTTTATAAATCTTTC
*Bam*HI-p27N114-2F	GGGGATCCGGATGAAACTCCAAAGGAGCGC
*Bam*HI-p27N21-F	GGGGATCCGGATGTTCAATCCAGGCAAAAT
*Bam*HI-p27N31-F	GGGGATCCGGATGTGCAACTTGGGTATAGA
*Bam*HI-p27N41-F	GGGGATCCGGATGTTTCGCAAGTGGTTCTT
p27N80-GFP-F	CTTCTGCAGCGGGGGCATGCATCATCATCATCATC
GFP-p27N80-R	GATGATGCATGCCCCCGCTGCAGAAGTCGTCGACT
p27N60-GFP-F	GGTGGATGCCTTCGGGGGCATGCATCATCATCATC
GFP-p27N60-R	GATGATGCATGCCCCCGAAGGCATCCACCGCCCAC
p27N50-GFP-F	TCTCAACTTTGGGGGCATGCATCATCATCATCATC
GFP-p27N50-R	GATGATGCATGCCCCCAAAGTTGAGACCAAAGAAC
p27N21–40GFP-F	TTGGAATCGCGGGGGCATGCATCATCATCATCATC
GFP-p27N21-40R	GATGATGCATGCCCCCGCGATTCCAACAGTCTATA
p27dAmph-F	GTCTGCAATCGATGCACATATGTGG
p27dAmph-R	ACATATGTGCATCGATTGCAGACAG
pUC*Sac*I-F	AATTTCACACAGGAAACAGC
FLAG-*Mlu*I-R	GGGGGACGCGTCTACTTGTCATCGTCGTCCTTGTAATC
L33A-F	TGCAATCTGCAACGCGGGTATAGAC
L33A-R	CCAACAGTCTATACCCGCGTTGCAG
I35A-F	CTGCAACTTGGGTGCAGACTGTTGG
I35A-R	GCGATTCCAACAGTCTGCACCCAAG
W38A-F	GGTATAGACTGTGCGAATCGCTTTC
W38A-R	CGAAAGCGATTCGCACAGTCTATAC
F41A-F	CTGTTGGAATCGCGCTCGCAAGTGG
F41A-R	AACCACTTGCGAGCGCGATTCCAAC
W44A-F	CGCTTTCGCAAGGCGTTCTTTGGTC
W44A-R	GAGACCAAAGAACGCCTTGCGAAAG
F45A-F	CTTTCGCAAGTGGGCCTTTGGTCTC
F45A-R	AGTTGAGACCAAAGGCCCACTTGCG
F46A-F	TCGCAAGTGGTTCGCTGGTCTCAAC
F46A-R	AAAGTTGAGACCAGCGAACCACTTG
L48A-F	TGGTTCTTTGGTGCCAACTTTGATG
L48A-R	TGCATCAAAGTTGGCACCAAAGAAC
F50A-F	TTCTTTGGTCTCAACGCTGATGCAC
F50A-R	ACATATGTGCATCAGCGTTGAGACC
W38A/F41A-F	GGTATAGACTGTGCGAATCGCGCTCGCAAGTGGTTC
W38A/F41A-R	GAACCACTTGCGAGCGCGATTCGCACAGTCTATACC

Biochemical treatment of membrane fractions

Biochemical treatment of membrane fractions prepared from *Agrobacterium*-infiltrated leaves (2 dai) was conducted as described previously (Mine et al., 2010a; Sanfaçon and Zhang, 2008).

In vitro transcription/RNA preparation

pRC2|G, pUCp27-FLAG, pUCp27-FLAG derivatives, and pUCp88 were digested with *Sma*I. The RNA transcripts were synthesized from these linearized templates in the presence of cap-structure analog (m7GpppG; New England Biolabs, Beverly, MA, USA), as described by Iwakawa et al. (2007, 2008), and purified on a Sephadex G-50 fine column (GE Healthcare). The RNA concentration was determined spectrophotometrically and its integrity was verified by 1% agarose gel electrophoresis in 0.5 × TBE buffer.

Evacuolated BY-2 protoplast lysate (BYL) experiments

Cell extracts of evacuolated BY-2 protoplasts were prepared as described by Komoda et al. (2004). The in vitro translation/replication reactions were conducted as previously described (Iwakawa et al., 2007; Mine et al., 2010b). Capped transcripts of p27-FLAG or its derivatives (200 ng) together with capped transcripts of p88 (100 ng) and RNA2 (500 ng) were added to each 50 μL BYL translation and replication mixture, followed by incubation at 17 °C for 4 h. Total proteins were analyzed by western blotting, as described previously (Mine et al., 2010a). Total RNAs were analyzed by northern blotting, as described previously (Iwakawa et al., 2007).

SDS-PAGE, BN/PAGE, and western blot analyses

SDS-PAGE, BN/PAGE, and western blot analyses were performed essentially as described by Mine et al. (2010a). Protein samples were analyzed on 12.5% (w/v) SDS-PAGE gel or on NativePAGE 4–16% Bis–Tris gel (Invitrogen, Carlsbad, CA, USA) and transferred onto a polyvinylidene fluoride (PVDF) microporous membranes (Immobilon-P Transfer Membrane; Millipore, Bedford, MA, USA). Rabbit polyclonal antibody raised against p27 (Takeda et al., 2005), anti-FLAG M2 monoclonal antibody (Sigma-Aldrich, St. Louis, MO, USA), and Living Colors A.v. Peptide antibody (Clontech Laboratories, Mountain View, CA, USA) were used as the primary antibodies. Alkaline phosphatase (AP)-conjugated anti-rabbit IgG antibody (Cell Signaling Technology, Beverly, MA, USA) and AP-conjugated anti-mouse IgG antibody (Kirkegaard and Perry Laboratories, Gaithersburg, MD, USA) were

used as secondary antibodies. The labeled proteins were visualized using a CDP-star chemiluminescence detection kit (Roche Applied Science) and the signals were detected with a luminescent image analyzer (LAS 1000plus; Fuji Photo Film, Tokyo, Japan).

Northern blot analysis

Total RNA of *Agrobacterium*-infiltrated leaves (2 dai) was isolated using PureLink Plant RNA Reagent (Invitrogen). Total RNA samples were analyzed on an Amersham Hybond-N^+ membrane (GE Healthcare) by northern blot analysis using digoxigenin (DIG)-labeled RNA probes specific for RCNMV positive- and negative-strand RNA2 as previously described (Iwakawa et al., 2007).

Reverse transcription polymerase chain reaction (RT-PCR)

Total RNA isolated from *Agrobacterium*-infiltrated leaves expressing GFP-p27 or p27-GFP in the presence of p88 and RNA2 were subjected to RT-PCR using SuperScript III Reverse Transcriptase (Invitrogen) and a primer set of Bam/sGFP-R and p27/sGFP-L. The PCR products were verified by 1% agarose gel electrophoresis in 1 × TAE buffer.

Acknowledgments

The authors thank to S. A. Lommel for the original RNA1 and RNA2 cDNA clones of RCNMV Australian strain. This work was supported in part by a Grant-in-Aid for Scientific Research (A) (18208004) and by a Grant-in-Aid for Scientific Research (A) (22248002) from the Japan Society for the Promotion of Science.

References

Ahlquist, P., Noueiry, A.O., Lee, W.M., Kusher, D.B., Dye, B.T., 2003. Host factors in positive-strand RNA virus genome replication. J. Virol. 77, 8181–8186.

Brass, V., Bieck, E., Montserret, R., Wölk, B., Hellings, J.A., Blum, H.E., Penin, F., Moradpour, D., 2002. An amino-terminal amphipathic α-helix mediates membrane association of the Hepatitis C virus nonstructural protein 5A. J. Biol. Chem. 277, 8130–8139.

Cole, C., Barber, J.D., Barton, G.J., 2008. The Jpred 3 secondary structure prediction server. Nucleic Acids Res. 36 (Web Server issue), W197–201.

den Boon, J.A., Chen, J., Ahlquist, P., 2001. Identification of sequences in *Brome mosaic virus* replicase protein 1a that mediate association with endoplasmic reticulum membranes. J. Virol. 75, 12370–12381.

den Boon, J.A., Diaz, A., Ahlquist, P., 2010. Cytoplasmic viral replication complexes. Cell Host Microbe 8, 77–85.

dos Reis Figueira, A., Golem, S., Goregaoker, S.P., Culver, J.N., 2002. A nuclear localization signal and a membrane association domain contribute to the cellular localization of the *Tobacco mosaic virus* 126 kDa replicase protein. Virology 301, 81–89.

Echeverri, A.C., Dasgupta, A., 1995. Amino terminal regions of poliovirus 2C protein mediate membrane binding. Virology 208, 540–553.

Gouttenoire, J., Penin, F., Moradpour, D., 2010. Hepatitis C virus nonstructural protein 4B: a journey into unexplored territory. Rev. Med. Virol. 20, 117–129.

Hwang, Y.T., McCartney, A.W., Gidda, S.K., Mullen, R.T., 2008. Localization of the Carnation Italian ringspot virus replication protein p36 to the mitochondrial outer membrane is mediated by an internal targeting signal and the TOM complex. BMC Cell Biol. 9, 54.

Hyodo, K., Mine, A., Iwakawa, H.O., Kaido, M., Mise, K., Okuno, T., 2011. Identification of amino acids in auxiliary replicase protein p27 critical for its RNA-binding activity and the assembly of the replicase complex in *Red clover mosaic necrotic virus*. Virology 413, 300–309.

Iwakawa, H.O., Kaido, M., Mise, K., Okuno, T., 2007. *cis*-Acting core RNA elements required for negative-strand RNA synthesis and cap-independent translation are separated in the 3'-untranslated region of *Red clover necrotic mosaic virus* RNA1. Virology 369, 168–181.

Iwakawa, H.O., Mizumoto, H., Nagano, H., Imoto, Y., Takigawa, K., Sarawaneeyaruk, S., Kaido, M., Mise, K., Okuno, T., 2008. A viral noncoding RNA generated by *cis* element-mediated protection against 5'→3'RNA decay represses both cap independent and cap-dependent translation. J. Virol. 82, 10162–10174.

Iwakawa, H.O., Mine, A., Hyodo, K., An, M., Kaido, M., Mise, K., Okuno, T., 2011. Template recognition mechanisms by replicase proteins differ between bipartite positive-strand genomic RNAs of a plant virus. J. Virol. 85, 497–509.

Kaido, M., Tsuno, Y., Mise, K., Okuno, T., 2009. Endoplasmic reticulum targeting of the *Red clover necrotic mosaic virus* movement protein is associated with the replication of viral RNA1 but not that of RNA2. Virology 395, 232–242.

Kaido, M., Funatsu, N., Tsuno, Y., Mise, K., Okuno, T., 2011. Viral cell-to-cell movement requires formation of cortical punctate structures containing *Red clover necrotic mosaic virus* movement protein. Virology 413, 205–215.

Kim, K.H., Lommel, S.A., 1994. Identification and analysis of the site of −1 frameshifting in *Red clover necrotic mosaic virus*. Virology 200, 574–582.

Komoda, K., Naito, S., Ishikawa, M., 2004. Replication of plant RNA virus genomes in a cell-free extract of evacuolated plant protoplast. Proc. Natl. Acad. Sci. USA 101, 1863–1867.

Koonin, E.V., 1991. The phylogeny of RNA-dependent RNA polymerases of positive strand RNA viruses. J. Gen. Virol. 72, 2197–2206.

Liu, L., Westler, W.M., den Boon, J.A., Wang, X., Diaz, A., Steinberg, H.A., Ahlquist, P., 2009. An amphipathic α-helix controls multiple roles of *Brome mosaic virus* protein 1a in RNA replication complex assembly and function. PLoS Pathogens 5 (3), e1000351, http://dx.doi.org/10.1371/journal.ppat.1000351.

Lommel, S.A., Weston-Fina, M., Xiong, Z., Lomonossoff, G.P., 1988. The nucleotide sequence and gene organization of *Red clover necrotic mosaic virus* RNA-2. Nucleic Acids Res. 16, 8587–8602.

McCartney, A.W., Greenwood, J.S., Fabian, M.R., White, K.A., Mullen, R.T., 2005. Localization of the Tomato bushy stunt virus replication protein p33 reveals a peroxisome-to-endoplasmic reticulum sorting pathway. Plant Cell 17, 3513–3531.

Miller, S., Krijnse-Locker, J., 2008. Modification of intracellular membrane structures for virus replication. Nat. Rev. Microbiol. 6, 363–374.

Mine, A., Takeda, A., Taniguchi, T., Taniguchi, H., Kaido, M., Mise, K., Okuno, T., 2010a. Identification and characterization of the 480 kDa template-specific RNA-dependent RNA polymerase complex of *Red clover necrotic mosaic virus*. J. Virol. 84, 6070–6081.

Mine, A., Hyodo, K., Takeda, A., Kaido, M., Mise, K., Okuno, T., 2010b. Interactions between p27 and p88 replicase proteins of *Red clover necrotic mosaic virus* play an essential role in viral RNA replication and suppression of RNA silencing via the 480 kDa viral replicase complex assembly. Virology 407, 213–224.

Mizumoto, H., Tatsuta, M., Kaido, M., Mise, K., Okuno, T., 2003. Cap-independent translational enhancement by the 3' untranslated region of *Red clover necrotic mosaic virus* RNA1. J. Virol. 77, 12113–12121.

Moradpour, D., Brass, V., Bieck, E., Friebe, P., Gosert, R., Blum, H.E., Bartenschlager, R., Penin, F., Lohmann, V., 2004. Membrane association of the RNA-dependent RNA polymerase is essential for Hepatitis C virus RNA replication. J. Virol. 78, 13278–13284.

Nagy, P.D., Pogany, J., 2008. Multiple roles of viral replication proteins in plant rna virus replication. In: Foster, G.D., Johansen, I.E., Hong, Y., Nagy, P.D. (Eds.), Plant Virology Protocols: From Viral Sequence to Protein Function. Humana Press, New Jersey, pp. 55–68.

Nagy, P.D., Pogany, J., 2012. The dependence of viral RNA replication on co-opted host factors. Nat. Rev. Microbiol. 10, 137–149.

Navarro, B., Rubino, L., Russo, M., 2004. Expression of the *Cymbidium ringspot virus* 33 kDa protein in *Saccharomyces cerevisiae* and molecular dissection of the peroxisomal targeting signal. J. Virol. 78, 4744–4752.

Okamoto, K., Nagano, H., Iwakawa, H.O., Mizumoto, H., Takeda, A., Kaido, M., Mise, K., Okuno, T., 2008. *cis*-preferential requirement of a-1 frameshift product p88 for the replication of *Red clover necrotic mosaic virus* RNA1. Virology 375, 205–212.

Panavas, T., Hawkins, C.M., Panaviene, Z., Nagy, P.D., 2005. The role of the p33: p33/p92 interaction domain in RNA replication and intracellular localization of p33 and p92 proteins of *Cucumber necrosis tombusvirus*. Virology 338, 81–95.

Prod'homme, D., Jakubiec, A., Tournier, V., Drugeon, G., Jupin, I., 2003. Targeting of the *Turnip yellow mosaic virus* 66 K replication protein to the chloroplast envelope is mediated by the 140 K protein. J. Virol. 77, 9124–9135.

Ritzenthaler, C., Elamawi, R., 2006. The ER in replication of positive-strand RNA viruses. In: Robinson, D.G. (Ed.), The Plant Endoplasmic Reticulum, Plant Cell Monographs, 4. Springer-Verlag, pp. 309–330.

Rubino, L., Weber-Lotfi, F., Dietrich, A., Stussi-Garaud, C., Russo, M., 2001. The open reading frame 1-encoded '36K' protein of *Carnation Italian ringspot virus* localizes to mitochondria. J. Gen. Virol. 82, 29–34.

Salonen, A., Ahola, T., Kääriäinen, L., 2005. Viral RNA replication in association with cellular membranes. Curr. Top. Microbiol. Immunol. 285, 139–173.

Sanfaçon, H., Zhang, G., 2008. Analysis of interactions between viral replicase proteins and plant intracellular membranes. In: Foster, G.D., Johansen, I.E., Hong, Y., Nagy, P.D. (Eds.), Plant Virology Protocols: From Viral Sequence to Protein Function. Humana Press, New Jersey, pp. 361–375.

Schaad, M.C., Jensen, P.E., Carrington, J.C., 1997. Formation of plant RNA virus replication complexes on membranes: role of an endoplasmic reticulum-targeted viral protein. EMBO J. 16, 4049–4059.

Schiffer, M., Edmundson, A.B., 1967. Use of helical wheels to represent the structures of proteins and to identify segments with helical potential. Biophys. J. 7, 121–135.

Schmidt-Mende, J., Bieck, E., Hugle, T., Penin, F., Rice, C.M., Blum, H.E., Moradpour, D., 2001. Determinants for membrane association of the Hepatitis C virus RNA-dependent RNA polymerase. J. Biol. Chem. 276, 44052–44063.

Schwartz, M., Chen, J., Janda, M., Sullivan, M., den Boon, J., Ahlquist, P., 2002. A positive-strand RNA virus replication complex parallels form and function of retrovirus capsids. Mol. Cell 9, 505–514.

Schwartz, M., Chen, J., Lee, W.M., Janda, M., Ahlquist, P., 2004. Alternate, virus-induced membrane rearrangements support positive-strand RNA virus genome replication. Proc. Natl. Acad. Sci. USA 101, 11263–11268.

Spuul, P., Salonen, A., Merits, A., Jokitalo, E., Kääriäinen, L., Ahola, T., 2007. Role of the amphipathic peptide of *Semliki Forest virus* replicase protein nsP1 in membrane association and virus replication. J. Virol. 81, 872–883.

Tajima, Y., Iwakawa, H.O., Kaido, M., Mise, K., Okuno, T., 2011. A long-distance RNA-RNA interaction plays an important role in programmed –1 ribosomal frameshifting in the translation of p88 replicase protein of *Red clover necrotic mosaic virus*. Virology 417, 169–178.

Takeda, A., Tsukuda, M., Mizumoto, H., Okamoto, K., Kaido, M., Mise, K., Okuno, T., 2005. A plant RNA virus suppresses RNA silencing through viral RNA replication. EMBO J. 24, 3147–3157.

Teterina, N.L., Gorbalenya, A.E., Egger, D., Bienz, K., Ehrenfeld, E., 1997. Poliovirus 2C protein determinants of membrane binding and rearrangements in mammalian cells. J. Virol. 71, 8962–8972.

Towner, J., Semler, B.L., 1996. Determinants of membrane association on poliovirus protein 3AB. J. Biol. Chem. 271, 26810–26818.

Turner, K.A., Sit, T.L., Callaway, A.S., Allen, N.S., Lommel, S.A., 2004. *Red clover necrotic mosaic virus* replication proteins accumulate at the endoplasmic reticulum. Virology 320, 276–290.

Van Wynsberghe, P.M., Chen, H.R., Ahlquist, P., 2007. Nodavirus RNA replication protein A induces membrane association of genomic RNA. J. Virol. 81, 4633–4644.

Wang, X., Lee, W., Watanabe, T., Schwartz, M., Janda, M., Ahlquist, P., 2005. *Brome mosaic virus* 1a nucleoside triphosphatase/helicase domain plays crucial roles in recruiting RNA replication templates. J. Virol. 79, 13747–13758.

Weber-Lotfi, F., Dietrich, A., Russo, M., Rubino, L., 2002. Mitochondrial targeting and membrane anchoring of a viral replicase in plant and yeast cells. J. Virol. 76, 10485–10496.

Xiong, Z., Lommel, S.A., 1989. The complete nucleotide sequence and genome organization of *Red clover necrotic mosaic virus* RNA-1. Virology 171, 543–554.

Xiong, Z., Lommel, S.A., 1991. *Red clover necrotic mosaic virus* infectious transcripts synthesized in vitro. Virology 182, 388–392.

Xiong, Z., Kim, K.H., Giesman-Cookmeyer, D., Lommel, S.A., 1993. The roles of the *Red clover necrotic mosaic virus* capsid and cell-to-cell movement proteins in systemic infection. Virology 192, 27–32.

Yamaga, A.K., Ou, J-h., 2002. Membrane topology of the Hepatitis C virus NS2 protein. J. Biol. Chem. 277, 33228–33234.

Zavriev, S.K., Hickey, C.M., Lommel, S.A., 1996. Mapping of the *Red clover necrotic mosaic virus* subgenomic RNA. Virology 216, 407–410.

Zhang, S.C., Zhang, G., Yang, L., Chisholm, J., Sanfaçon, H., 2005. Evidence that insertion of Tomato ringspot nepovirus NTB-VPg protein in endoplasmic reticulum membranes is directed by two domains: a C-terminal transmembrane helix and an N-terminal amphipathic helix. J. Virol. 79, 11752–11765.

Zhang, G., Sanfaçon, H., 2006. Characterization of membrane association domains within the *Tomato ringspot nepovirus* X2 protein, an endoplasmic reticulum-targeted polytopic membrane protein. J. Virol. 80, 10847–10857.